1521-0111/88/2/316–325$25.00
MOLECULAR PHARMACOLOGY

http://dx.doi.org/10.1124/mol.114.097345
Mol Pharmacol 88:316–325, August 2015

Identification of a Dual Inhibitor of SRPK1 and CK2 That Attenuates Pathological Angiogenesis of Macular Degeneration in Mice[S]

Satoshi Morooka, Mitsuteru Hoshina, Isao Kii, Takayoshi Okabe, Hirotatsu Kojima, Naoko Inoue, Yukiko Okuno, Masatsugu Denawa, Suguru Yoshida, Junichi Fukuhara, Kensuke Ninomiya, Teikichi Ikura, Toshio Furuya, Tetsuo Nagano, Kousuke Noda, Susumu Ishida, Takamitsu Hosoya, Nobutoshi Ito, Nagahisa Yoshimura, and Masatoshi Hagiwara

Department of Ophthalmology and Visual Sciences (S.M., N.Y.), Department of Anatomy and Developmental Biology (S.M., I.K., Ke.N., Ma.H.), and Medical Research Support Center (Y.O., M.D.), Graduate School of Medicine, Kyoto University, Kyoto, Japan; Laboratory of Structural Biology, Medical Research Institute (Mi.H., No.I., T.I.), and Laboratory of Chemical Bioscience, Institute of Biomaterials and Bioengineering (S.Y., T.H.), Tokyo Medical and Dental University, Tokyo, Japan; Open Innovation Center for Drug Discovery, The University of Tokyo, Tokyo, Japan (T.O., H.K., T.N.); PharmaDesign, Inc., Tokyo, Japan (Na.I., T.F.); and Department of Ophthalmology, Graduate School of Medicine, Hokkaido University, Sapporo, Japan (J.F., Ko.N., S.I.)

Received December 8, 2014; accepted May 20, 2015

ABSTRACT

Excessive angiogenesis contributes to numerous diseases, including cancer and blinding retinopathy. Antibodies against vascular endothelial growth factor (VEGF) have been approved and are widely used in clinical treatment. Our previous studies using SRPIN340, a small molecule inhibitor of SRPK1 (serine-arginine protein kinase 1), demonstrated that SRPK1 is a potential target for the development of antiangiogenic drugs. In this study, we solved the structure of SRPK1 bound to SRPIN340 by X-ray crystallography. Using pharmacophore docking models followed by in vitro kinase assays, we screened a large-scale chemical library, and thus identified a new inhibitor of SRPK1. This inhibitor, SRPIN803, prevented VEGF production more effectively than SRPIN340 owing to the dual inhibition of SRPK1 and CK2 (casein kinase 2). In a mouse model of age-related macular degeneration, topical administration of eye ointment containing SRPIN803 significantly inhibited choroidal neovascularization, suggesting a clinical potential of SRPIN803 as a topical ointment for ocular neovascularization. Thus SRPIN803 merits further investigation as a novel inhibitor of VEGF.

Introduction

Angiogenesis is an important biologic phenomenon, not only in physiologic conditions including embryogenesis, skeletal growth, and wound healing, but also in pathologic conditions such as tumor growth, chronic inflammatory disorders, and intraocular neovascular diseases (Maharaj and D'Amore, 2007). Vascular endothelial growth factor (VEGF), a mitogen for endothelial cells, is a key regulator of angiogenesis associated with various pathologic conditions (Ferrara et al., 2003; Okabe et al., 2014). VEGF binds VEGF receptor and activates its tyrosine kinase activity, which in turn triggers the mitogen-activated protein kinase signaling cascade (Fukuda et al., 2002), leading to endothelial cell proliferation and neovascularization (Xu et al., 2008). Because of the importance of VEGF in these processes, drugs targeting VEGF have been developed: For example, an antibody against VEGF, bevacizumab (Avastin), was first approved for patients with metastatic colorectal cancer (Hurwitz et al., 2004). Anti-VEGF antibodies have the potential to be of therapeutic value for a variety of angiogenic disorders.

Anti-VEGF antibodies, including ranibizumab (Lucentis) (Rosenfeld et al., 2006), pegaptanib (Macugen) (Gragoudas et al., 2004), and anti-VEGF decoy receptor of aflibercept (Eylea) (Heier et al., 2012), have also been approved for intraocular neovascularization. Age-related macular degeneration (AMD) is one of the most common diseases of intraocular neovascularization, the leading cause of blindness (Ferris et al., 1984; Klein et al., 1995; Seddon and Chen, 2004). Intravitreous injection of anti-VEGF antibodies has been demonstrated to cure AMD; however, this therapy increases the risk of several

This work was supported by Target Protein Research Programs of the Ministry of Education, Culture, Sports, Science and Technology of Japan; Grants-in-Aid from the National Institute of Biochemical Innovation of Japan [Grants 12-03]; and Platform for Drug Discovery, Informatics, and Structural Life Science from the Ministry of Education, Culture, Sports, Science and Technology, Japan.
dx.doi.org/10.1124/mol.114.097345.
[S] This article has supplemental material available at molpharm.aspetjournals.org.

ABBREVIATIONS: AMD, age-related macular degeneration; DMSO, dimethyl sulfoxide; PCR, polymerase chain reaction; siRNA, small interfering RNA; VEGF, vascular endothelial growth factor.

complications, including infection, inflammation, higher intraocular pressure, and vitreous hemorrhage (Shima et al., 2008; Ventrice et al., 2013). Therefore, there is an urgent need for new therapeutics using small molecules that can be safely and easily administered, such as eye drops and ointments. Small-molecule inhibitors of angiogenesis would also contribute to therapies against other angiogenic diseases.

In a previous study, we demonstrated the antiangiogenic activity of SRPIN340, a small molecule that was developed as an inhibitor of serine-arginine protein kinase 1 (SRPK1) (Fukuhara et al., 2006). SRPK1 phosphorylates serine/arginine-rich proteins and regulates splicing and transcription (Ngo et al., 2005; Nishida et al., 2011; Ogawa and Hagiwara, 2012), and also phosphorylates peroxisome proliferator-activated receptor-γ coactivator 1 (PGC1), hepatitis B virus core protein, and eukaryotic translation initiation factor 4 γ (eIF4G) to regulate glucogenesis (Lin et al., 2005; Nikolakaki et al., 2008), viral replication (Daub et al., 2002), and mTOR signaling (Hu et al., 2012), respectively. SRPK1 inhibition prevents pathologic angiogenesis, and suppresses angiogenesis-associated tumor growth (Amin et al., 2011) and pathologic choroidal neovascularization in animal models (Dong et al., 2013). Inversely, aberrant SRPK1 expression induces constitutive Akt activation, leading to cancer progression (Wang et al., 2014). Thus, SRPK1 represents a potent drug target for treatment of pathologic angiogenesis.

Here, we report the application of a computational protocol based on molecular docking and dynamics simulations, combined with a pharmacophore-based database search, to identify compounds of interest. Using this method, we identified a new small molecule, SRPIN803, that inhibits VEGF production. In vitro kinase profiling revealed that SRPIN803 inhibited casein kinase 2 (CK2) as well as SRPK1. The dual inhibition of SRPK1 and CK2 were predicted to synergistically suppress VEGF production. In a mouse model, topical administration of SRPIN803 suppressed intraocular neovascularization. Thus, SRPIN803 represents a candidate therapeutic drug for treatment of pathologic angiogenesis.

Materials and Methods

Crystallographic Study. Crystals of the kinase fragment of SRPK1 (residues 42–255 and 474–655) were obtained according to a previously reported method (Ngo et al., 2007) with some modifications. The SRPIN340 complex was obtained by soaking crystals of apo-SRPK1 in mother liquor containing the inhibitor.

The diffraction data set was obtained at 100 K from a single crystal at BL38B1 of SPring-8 (Harima, Japan). The 2.0-Å diffraction data were integrated and scaled using the program HKL2000 (HKL Research Inc., Charlottesville, VA). The space group was $P6_522$, with unit cell parameters $a = b = 75.1$ Å and $c = 310.6$ Å.

Structure determination and refinement were performed using the CCP4 suite (Winn et al., 2011). The structure was solved by molecular replacement using a previously reported structure of SRPK1 [PDB ID 1WAK; (Ngo et al., 2007)] and refined by REFMAC (Murshudov et al., 2011). The graphics software Coot was used for model building (Emsley et al., 2010). Some of the statistics of data collection and structure refinement are shown in Supplemental Table 1. Figures were created using the PyMOL Molecular Graphics System (Version 1.5.0.4; Schrödinger, New York, NY). Coordinates and structure factors of the complex were deposited in the Protein Data Bank (PDB ID 4WUA).

Docking Simulation. The model of SRPIN803 in complex with CK2α was obtained using AutoDock Vina (Trott and Olson, 2010). The crystal structure of the inhibitor complex of CK2α (PDB ID 1M2Q; De Moliner et al., 2003) was used as the protein model after removal of the ligand and inhibitor molecules. The docking simulation was performed around the ATP-binding pocket of CK2α. The model of SRPIN803 in complex with SRPK1 was obtained in a similar manner, using our X-ray structure as the protein model. The coordinates of the models can be found in the Supplemental Material. The result was visualized using Discovery Studio Visualizer (Accelrys Inc., Cambridge, UK).

Cell Culture. ARPE-19 cells, a spontaneously arising human retinal pigment epithelial cell line, were purchased from the American Type Culture Collection (Manassas, VA) and maintained at 37°C in a 5% CO_2/air incubator in Dulbecco's modified Eagle's medium/Ham's F-12 (Nacalai Tesque, Kyoto, Japan) supplemented with 10% fetal bovine serum (Sigma-Aldrich, St. Louis, MO) and 1% Penicillin-Streptomycin Mixed Solution (Nacalai Tesque).

Small Interfering RNA. Stealth small interfering RNAs (siRNAs; Life Technologies, Grand Island, NY) were diluted with OptiMEM (Life Technologies), and incubated with Lipofectamine RNAiMAX (Life Technologies). ARPE-19 cells were seeded onto 12-well plates at 50,000 cells/well, and then transfected with siRNAs (final concentration, 10 nM) against *SRPK1*, *CK2A1*, *CK2A2*, or *Luciferase*. Analyses were performed 48 hours post-transfection. Product names of the siRNAs used were as follows: *SRPK1* (SRPK1-HSS110210), *CK2A1* (CSNK2A1-HSS175396), *CK2A2* (CSNK2A2-HSS102398), and Luciferase (Life Technologies).

Reverse Transcription, Semiquantitative, and Quantitative Polymerase Chain Reaction. Total RNA was purified from cells using the RNeasy kit (QIAGEN, Hilden, Germany). Purified RNA was converted into cDNA using SuperScript II (Life Technologies) with anchored oligo-dT primer (Life Technologies).

ExTaq (TaKaRa Bio, Otsu, Japan) was used for semiquantitative polymerase chain reaction (PCR) analysis. The reaction was carried out using the following cycle: 95°C for 20 seconds, 58°C for 20 seconds, and 72°C for 60 seconds, for 25–35 cycles. Primer sequences are listed in Supplemental Table 5. PCR products were separated by electrophoresis and stained with ethidium bromide (Nacalai Tesque). Images were obtained using a ChemiDoc XRS System (Bio-Rad Laboratories, Hercules, CA).

Quantitative PCR was performed using SYBR Premix Ex Taq (TaKaRa Bio) on a real-time PCR cycler (StepOnePlus; Life Technologies). The human *GAPDH* gene was used to normalize the input cDNA. Sequences of the primers are listed in Supplemental Table 6. All cDNA samples were tested in duplicate, and the average values were used in statistical analysis.

Enzyme-Linked Immunosorbent Assay. ARPE-19 cells were seeded at a density of 1×10^4 cells/well in 12-well plates and cultured for 24 hours. The culture medium was replaced with Dulbecco's modified Eagle's medium supplemented with 1% fetal bovine serum 24 hours before treatment with compounds. The cells were treated with 1 nM tumor growth factor β (R&D Systems/Bio-Techne, Minneapolis, MN). Culture supernatants were collected 24 or 72 hours after the treatment, and VEGF levels in the supernatants were determined using an enzyme-linked immunosorbent assay kit (R&D Systems).

In Vitro Kinase Assay. Recombinant human SRPK1 protein was purified from *Escherichia coli* (Fukuhara et al., 2006). The in vitro kinase assay was performed as described previously (Fukuhara et al., 2006) with some modifications. The SRPK1 kinase reaction was performed in a reaction mixture containing serially diluted inhibitors, 10 mM 4-morpholinepropanesulfonic acid-KOH (pH 7.0), 10 mM magnesium acetate, 200 μM EDTA, 1 μM ATP, 0.017 mg/ml RS peptide, and recombinant SRPK1 in a final volume of 25 μl. The final concentration of dimethyl sulfoxide (DMSO) was adjusted to 0.1 or 1%, regardless of the inhibitor concentration.

Human recombinant casein kinase 2 (CK2) was purchased from New England Biolabs (Ipswich, MA). The CK2 kinase reaction was performed in a reaction mixture containing serially diluted inhibitors, 20 mM Tris-HCl (pH 7.5), 50 mM potassium chloride, 10 mM

magnesium chloride, 20 μM ATP, 0.02 mg/ml CK2 substrate (Sigma-Aldrich), and 625 IU of recombinant CK2 in a final volume of 25 μl. The final concentration of DMSO was adjusted to 1%, regardless of the inhibitor concentration.

The reaction mixture was incubated at 30°C for 15 minutes, and residual ATP was measured using Kinase-Glo (Promega, Madison, WI).

$$\text{Relative kinase Activity}(\%) = (C - A)/(C - B) \times 100 \quad (1)$$

where A = count per second (CPS) from the reaction with an inhibitor, B = CPS from the reaction with 1% DMSO, and C = CPS from the reaction without enzyme (background).

Laser-Induced Choroidal Neovascularization in Mice. All animal experiments were approved by the Kyoto University Animal Use Committee and conducted in accordance with the Association for Research in Vision and Ophthalmology Statement for the Use of Animals in Ophthalmic and Vision Research. Six- to eight-week-old C57BL/6J male mice (Japan SLC, Tokyo, Japan) were used for this study. Anesthesia was induced by intraperitoneal injection of ketamine (100 mg/kg body weight) and xylazine (10 mg/kg body weight), and pupils were dilated by topical administration with 5% phenylephrine hydrochloride and 5% tropicamide. After anesthesia and pupil dilation, four laser spots were placed around the optic disc (532 nm, 150 mW power, 0.1 seconds, spot size 75 μm in diameter; Novus Spectra, Lumenis, Tokyo, Japan) using a slit-lamp delivery system with a cover glass as a contact lens.

Intravitreous Injection. Each compound (50 mM in DMSO) was diluted with phosphate-buffered saline to various concentrations (final 0.1% DMSO) just before injection. Immediately after laser photocoagulation, 1.0 μl of the diluted solution was injected into the vitreous body using a 33-gauge needle (Extreme Microsyringe; Ito Corporation, Tokyo, Japan).

Administration of the Ointment. SRPIN803 was formulated into an ointment base containing fluid paraffin and white Vaseline to a final concentration of 10%. The ointment base alone was used as a negative control. These ointments were partitioned into 1.5-ml tubes and stored in the dark at room temperature. The ointment (7.0 μl) was applied to both eyes of the model mice, 3 times per day for 7 days, using a Microman (Gilson, Middleton, WI).

Measurement of the Neovascularization Area. Seven days after laser-induced photocoagulation, model mice were euthanized by anesthesia and perfused with 1 ml of 0.5% fluorescein isothiocyanate–labeled dextran (Sigma-Aldrich). Flat mounts of retinal pigment epithelium and choroid were obtained by removing the anterior segments and the neural retina. Four to six radial relaxing incisions were made to allow the residual posterior eyecup to be laid flat. After mounting with Aqua-Poly/Mount (Polysciences, Warrington, PA) and covering with a cover slip, the flat mounts were examined with a fluorescence microscope (Biorevo BZ-9000; Keyence, Osaka, Japan) and the area of neovascularization was measured and used for evaluation.

Results

SRPK1 Inhibition Potently Suppresses VEGF Production. Our previous report showed that SRPIN340 suppressed the level of VEGF mRNA in mouse retina (Dong et al., 2013). Gammons et al., 2014 reported that VEGF production was decreased in human skin melanoma cells (A375) infected with a lentivirus containing *SRPK1* shRNA. To confirm that inhibition of SRPK1 suppresses production of VEGF, we performed siRNA-mediated knockdown of *SRPK1* in the human retinal pigment epithelial cell line ARPE-19 (Supplemental Fig. 1A). *VEGF* mRNA expression and secreted VEGF protein in culture supernatants were measured by reverse transcription quantitative PCR and enzyme-linked immunosorbent assay, respectively. siRNA against the *luciferase* gene was used as a negative control. Treatment with siRNA against *SRPK1* suppressed the level of *VEGF* mRNA to 53% of the control ($P < 0.01$; Supplemental Fig. 1B) and decreased the level of secreted VEGF protein to 36% of the control ($P < 0.01$; Supplemental Fig. 1C). These results are consistent with previous studies showing that SRPIN340 suppresses VEGF production (Dong et al., 2013), and validated our strategy of targeting SRPK1 to develop novel antiangiogenic treatments.

Crystal Structure of SRPK1 Bound with SRPIN340. Structural information about the binding mode of SRPIN340 in the ATP-binding pocket of SRPK1 will facilitate development of a new class of SRPK1 inhibitors. Hence, we cocrystalized the SRPK1/SRPIN340 complex and determined its structure by X-ray crystallography. Recombinant SRPK1 kinase domain was produced in *E. coli* and purified by immobilized nickel-chelate affinity chromatography, followed by gel-filtration chromatography. The crystals of SRPK1 were obtained from the purified protein and then soaked in a buffer containing SRPIN340. The X-ray crystallographic data are summarized in Supplemental Table 1. The crystallographic structure of the SRPK1/SRPIN340 complex is shown in Fig. 1A (PDB ID 4WUA). SRPIN340 binds SRPK1 at the ATP-binding cleft and forms extensive hydrophobic interactions with residues including Leu86, Val94, Phe165, Leu168, Leu220, Tyr231, and Leu231 (Fig. 1B). The oxygen atom of the carbonyl group of SRPIN340 fixes the position of the ligand by forming a hydrogen bond with the main-chain amide of Leu168 (Fig. 1B). Compared with the crystal structure of unliganded SRPK1 (PDB ID 1WAK), the Leu168–Gly169 peptide was flipped in the SRPK1/SRPIN340 complex (Fig. 1C), suggesting that peptide flipping was induced by the binding of SRPIN340 in the ATP-binding pocket. The trifluoromethyl group of SRPIN340 is located in the region occupied by the main-chain oxygen of Leu168 in the unliganded SRPK1 structure (Fig. 1C), suggesting that the bulky trifluoromethyl group pushes away the main chain of Leu168 and induces peptide flipping. Furthermore, the flipped main-chain oxygen of Leu168 forms a hydrogen bond with the main-chain nitrogen of Val223 (Fig. 1C), potentially stabilizing the flipped structure. These results demonstrate that SRPIN340 binds to the ATP-binding pocket and induces peptide flipping, which is probably required for potent inhibition of SRPK1.

In Silico and Subsequent In Vitro Screening of Chemical Inhibitors of SRPK1. To identify a new class of SRPK1 inhibitors, we screened a chemical library containing 71,955 chemical structures. Specifically, we performed a sequential screen consisting of an in silico docking study following by a pharmacophore search or similarity search of known inhibitors of CMGC family kinases, and selected the top 9511 compounds. These chemical compounds were then assessed by in vitro kinase assay using recombinant SRPK1 and its substrate. A summary of the in vitro screening results is provided in Fig. 2A. We selected the top three compounds that inhibit SRPK1 activity to <10% of the DMSO control. Two of these compounds possess scaffolds found in compounds that are frequently selected by screening (Baell and Holloway, 2010) and were consequently omitted. Thus, the strongest inhibitor was named SRPIN803 (Fig. 2B). SRPIN803 was resynthesized (Supplemental Material), and its activity and specificity were confirmed by in vitro kinase assay: The compound inhibited the in vitro activity of SRPK1 with an IC_{50} value of 2.4 μM but did not inhibit SRPK2 (Fig. 2C).

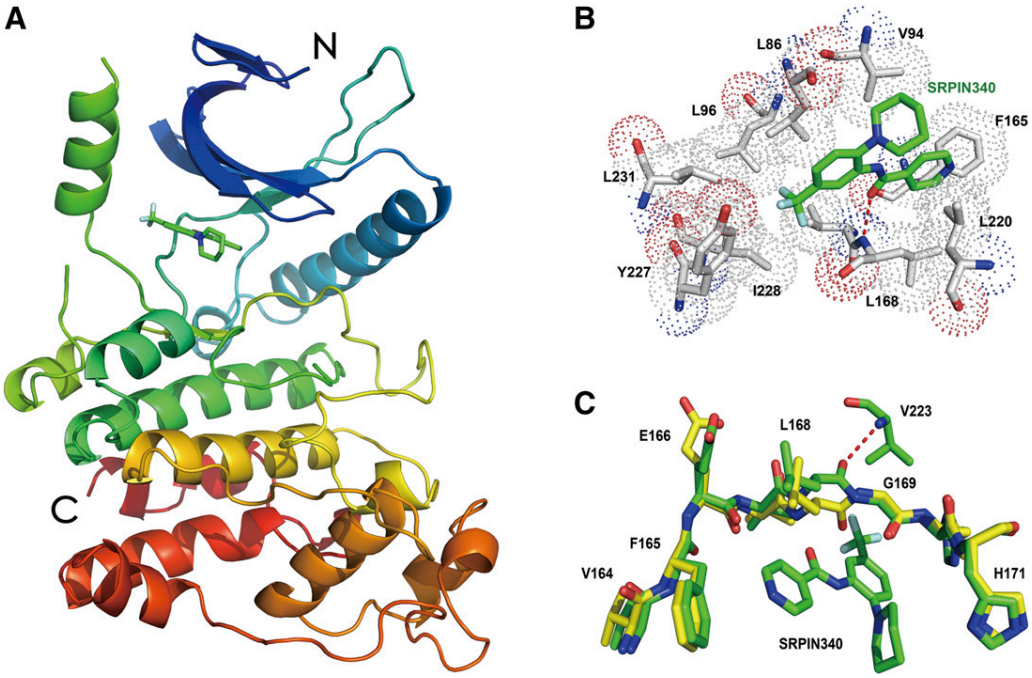

Fig. 1. Crystal structure of the SRPK1/SRPIN340 complex. (A) Overall structure. SRPK1 and SRPIN340 are shown in ribbon mode and stick mode, respectively. SRPIN340 binds to the ATP-binding pocket of SRPK1 (PDB ID 4WUA). C, carboxy terminus; N, amino terminus. (B) Stick representation of the inhibitor-binding site of the SRPK1/SRPIN340 complex. The red dotted line indicates a hydrogen bond. A space-filling model is illustrated by the dots surrounding the stick representation. (C) The peptide flip around Leu168–Gly169. Residues Val164–His171 and Val223 are shown in stick representation. The structures illustrated are SRPK1 without ligand (PDB ID 1WAK), shown in yellow, and SRPK1 with SRPIN340, shown in green. The red dotted line indicates a hydrogen bond.

To predict the binding mode of SRPIN803 to the ATP-binding pocket of SRPK1, we performed an in silico docking study. The simulation revealed that SRPIN803 interacts with the ATP-binding pocket, and that the trifluoromethyl group of SRPIN803 was located in the same region as in the SRPIN340/SRPK1 crystal structure (Fig. 2D).

SRPIN803 Suppresses VEGF Production. In the next step, we investigated whether SRPIN803 suppressed VEGF production in ARPE-19 cells. As we expected, treatment with SRPIN803 (10 μM) for 24 hours decreased the level of secreted VEGF protein in the culture supernatant relative to treatment with 0.1% DMSO ($P < 0.01$; Fig. 3A), with no cytotoxicity (Supplemental Fig. 2). In addition, treatment with SRPIN803 (10 μM) significantly suppressed the expression of *VEGF* mRNA to 48% of the control ($P < 0.01$; Fig. 3B), suggesting that SRPIN803 inhibited the expression of *VEGF* mRNA. Furthermore, treatment with SRPIN803 suppressed VEGF production in a dose- and time-dependent manner (Supplemental Fig. 3).

Next, we examined the effect of SRPIN803 on the transcriptome, using ARPE-19 cells treated with SRPIN803 (10 μM) for 4 hours. A summary of gene-expression array data are provided in Supplemental Fig. 3 (GEO accession number GSE62947; detailed data, Supplemental Table 2). mRNA levels of *VEGF* and 30 other genes were reduced by more than 1.8-fold (Supplemental Fig. 4). The downregulated genes included *IL8*, *HMOX1*, and *HK2*, which play a role in angiogenesis (Dulak et al., 2008; Martin et al., 2009; Wolf et al., 2011). Thus, SRPIN803 regulates expression of genes involved in angiogenesis.

Structural Requirement of SRPIN803. To confirm the structural requirements of SRPK1 inhibition by SRPIN803, we performed in vitro kinase assays and VEGF secretion assays using four derivative compounds of SRPIN803 in which the trifluoromethyl group was replaced. Substitutions of the trifluoromethyl group decreased both the inhibitory activity of SRPK1 and the suppression of VEGF production (Fig. 3C). These results demonstrated that the trifluoromethyl group of SRPIN803 plays a crucial role in both SRPK1 inhibition and the suppression of VEGF production. To further analyze the structural requirements for SRPK1 inhibition, we purchased compounds that were structurally similar to SRPIN803 and retained the trifluoromethyl group, and checked their SRPK1 inhibition. Structures of these compounds and inhibitory activities against SRPK1 were summarized in Supplemental Table 3. The derivatives that possess R2 groups similar to SRPIN803 inhibited SRPK1, though their inhibitory activities were weaker compared with SRPIN803. In contrast, the derivatives with larger or structurally different R2 groups did not inhibit SRPK1, as predicted by the docking simulation.

SRPIN803 Is a Dual Inhibitor of SRPK1 and CK2α1/2α2. To determine the kinase selectivity of SRPIN803, we assessed its inhibitory effect against a panel of 306 kinases. In these experiments, we used SRPIN803 at a concentration of 2.5 μM. Only two other kinases, CK2α1 and CK2α2, were inhibited by more than 50% (Fig. 4A; Supplemental Table 3). CK2α1 and CK2α2 form a tetrameric complex that constitutes the catalytic subunit of CK2 (Hathaway and Traugh, 1982; Meisner et al., 1989; Pinna, 1990). In the following experiments, we used the tetrameric complex of CK2. In the in vitro kinase assay, the IC_{50} value of SRPIN803 against CK2 was 203 nM (Fig. 4B). Thus, SRPIN803 is a dual inhibitor of

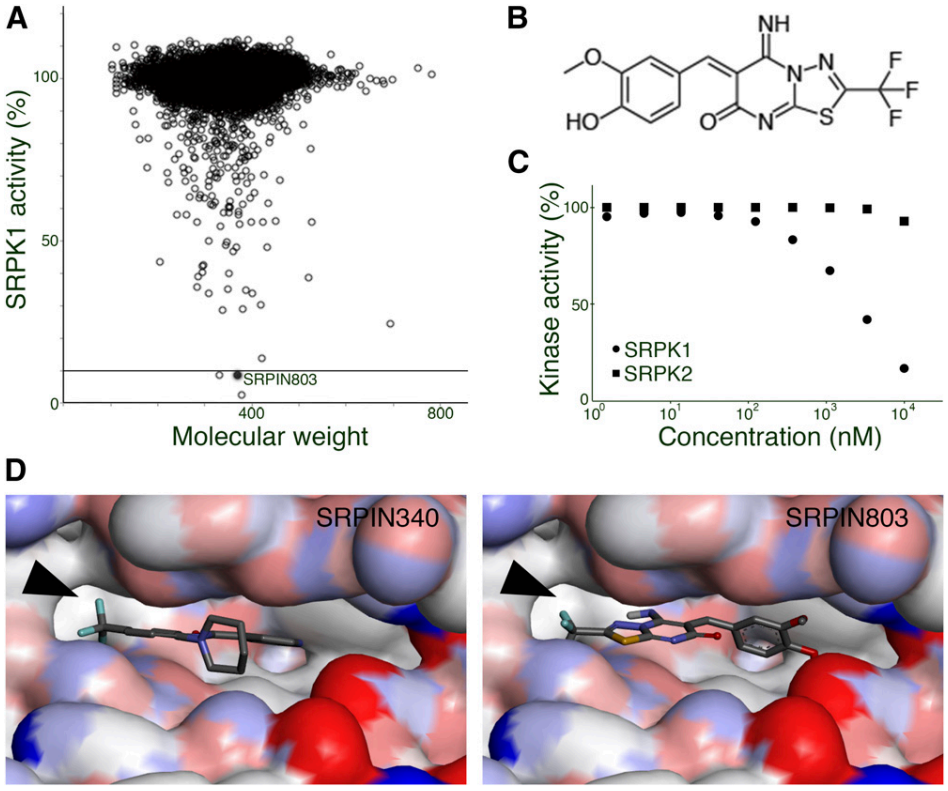

Fig. 2. Identification of SRPIN803 as an inhibitor of SRPK1. (A) Relative in vitro activities of SRPK1 in the presence of small molecules (10 μM). A total of 9511 compounds were screened. The top three compounds that inhibited SRPK1 activity to below 10% of the DMSO control are shown in the scatter plot. (B) Chemical structure referred to as SRPIN803. (C) SRPIN803 inhibits the kinase activity of SRPK1 with an IC_{50} value of 2.4 μM but does not inhibit SRPK2. (D) A docking model for SRPIN803 to SRPK1 (right, Supplemental PDB File 1), compared with the same view of the crystal structure of the SRPK1/SRPIN340 complex (left, PDB ID 4WUA). The arrowhead indicates the trifluoromethyl group.

SRPK1 and CK2. By contrast, SRPIN340 did not inhibit CK2 (Fig. 4B), suggesting that CK2 is also involved in the effective inhibition of VEGF production.

To verify inhibition of CK2 by SRPIN803, we performed an in silico docking simulation using the crystal structure of CK2α (PDB ID 1M2Q). The simulation revealed that SRPIN803 fits into the ATP-binding pocket of CK2α (Fig. 4C), whereas SRPIN340 does not fit (Supplemental Fig. 5), supporting the idea that SRPIN803 is the dual inhibitor of SRPK1 and CK2α.

CK2 Plays a Role in VEGF Production. CK2 is a ubiquitous serine/threonine kinase that phosphorylates and/or interacts with more than 300 substrates (Meggio and Pinna, 2003) and is involved in many central biologic processes (Litchfield, 2003; Olsten and Litchfield, 2004; Unger et al., 2004), including VEGF production (Noy et al., 2012a,b). Three inhibitors of CK2, 5,6-dichloro-1-β-D-ribofuranosylbenzimidazole, 4,5,6,7-tetrabromobenzotriazole, and apigenin, as well as overexpression of a dominant-negative mutant of CK2α, inhibit hypoxia-inducible factor-1 activity and consequently

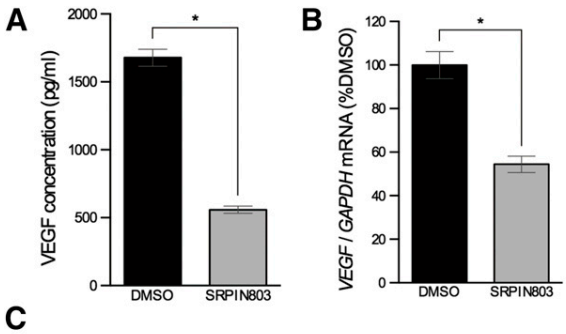

C

Compound No.		SRPIN803	SRPIN803a	SRPIN803b	SRPIN803c	SRPIN803d
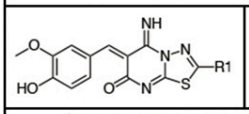	R1				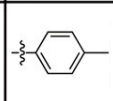	
SRPK1 activity (%)		19.1	50.4	64.7	81.2	88.0
VEGF protein level compared with control (%)		28.1	54.3	88.6	76.1	93.9

Fig. 3. SRPIN803 suppresses VEGF production. (A and B) Treatment with SRPIN803 decreases total VEGF protein and *VEGF* mRNA relative to the treatment with 0.1% DMSO. *$P < 0.01$. (A) Enzyme-linked immunosorbent assay (ELISA) of total VEGF protein in culture supernatants of ARPE-19 cells treated with SRPIN803 (10 μM) (mean ± S.E.M. of four independent experiments). (B) Quantitative PCR analysis of total *VEGF* mRNA of the ARPE-19 cells treated with SRPIN803 (10 μM) (mean ± S.E.M. of the results of four experiments performed in triplicate). (C) Structural requirements for SRPK1 inhibition by SRPIN803. The chemical structures of SRPIN803 and its derivatives are shown. IC_{50} values of these derivatives were calculated by in vitro kinase assay. The levels of secreted VEGF protein in culture supernatants of ARPE-19 cells treated with the derivatives (final concentration, 10 μM) were measured by ELISA.

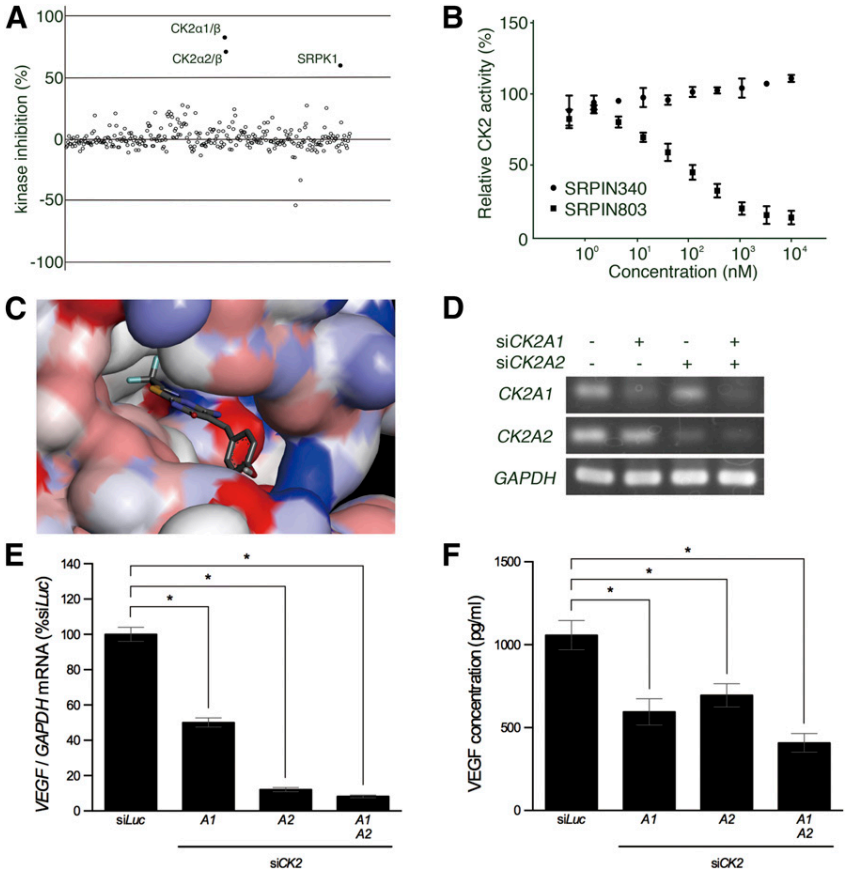

Fig. 4. SRPIN803 is a dual inhibitor of SRPK1 and CK2. (A) Scatter plots of the 306-kinase panel of SRPIN803 (2.5 μM). Black dots indicate greater than 50% inhibition. (B) SRPIN803 inhibited CK2 activity with an IC_{50} value of 203 nM, whereas SRPIN340 did not inhibit the enzyme. (C) A docking model of SRPIN803 bound to the ATP-binding pocket of CK2α (Supplemental PDB file 2). (D) Semiquantitative PCR analysis to determine expression of *CK2A1* and *CK2A2* in the ARPE-19 cells. siRNAs against *CK2A1* and *CK2A2* reduced the corresponding mRNA levels, relative to treatment with control siRNA against luciferase. *GAPDH* was used as an internal control. (E and F) Treatment with siRNA against either *CK2A1* or *CK2A2* significantly suppressed expression of *VEGF* mRNA and decreased the level of secreted VEGF protein, relative to the treatment with the control. $^*P < 0.01$. (E) Quantitative PCR analysis of total *VEGF* mRNA of the ARPE-19 cells transfected with siRNAs (means ± S.E.M. of the results from four experiments performed in duplicate). (F) Enzyme-linked immunosorbent assay of secreted VEGF protein in the culture supernatants of the ARPE-19 cells transfected with siRNAs (means ± S.E.M. of three independent experiments).

prevent induction of VEGF expression by hypoxia (Mottet et al., 2005).

To investigate whether CK2 inhibition contributes to reduction of VEGF production, we performed siRNA-mediated knockdown of *CK2A1* and *CK2A2* in ARPE-19 cells (Fig. 4D). Treatment with siRNA against either *CK2A1* or *CK2A2* significantly suppressed the expression of *VEGF* mRNA (Fig. 4E) and decreased the level of secreted VEGF protein (Fig. 4F) relative to the control. Furthermore, knockdown of both *CK2A1* and *CK2A2* increased the suppression of VEGF expression and secretion (Fig. 4, E and F). Thus, CK2 is also involved in VEGF production. Furthermore, the level of secreted VEGF protein was not significantly reduced by SRPIN803 in the codepleted cells of SRPK and CK2, relative to the control (Supplemental Fig. 6). Taken together, these findings indicate that the antiangiogenic effect of SPRIN803 is mediated by the dual inhibition of SRPK1 and CK2.

Intravitreous Injection of SRPIN803. As a result of the potent anti-VEGF activity of SRPIN803, we investigated whether SRPIN803 is an effective antiangiogenic drug in a mouse model. We performed laser photocoagulation to cause pathologic choroidal neovascularization beneath the retina, thereby generating a mouse model that recapitulates the pathogenesis of AMD (Aguilar et al., 2008). Just after the laser photocoagulation, we injected SRPIN803 once intravitreously. Seven days later, fluorescein isothiocyanate–dextran was injected into the left ventricle, and the eyes were enucleated, opened by incision, and laid flat. The flat-mounts of the eyes were visualized by fluorescence microscopy, and the areas of neovascularization were quantitated. The injection of SRPIN803 significantly decreased the neovascularization area, relative to DMSO injection ($P < 0.01$), in a dose-dependent manner (Fig. 5, A and B). SRPIN340 also decreased the area of neovascularization, but its activity was weaker than that of SRPIN803 (Supplemental Fig. 7).

To confirm reduction of inflammation-associated molecules following treatment with SRPIN803, as previously reported for SRPIN340 (Aguilar et al., 2008; Dong et al., 2013), we measured the levels of monocyte chemoattractant protein-1 (MCP1) and intercellular adhesion molecule-1 (ICAM1) in retinal pigment epithelium and choroid 3 days after laser photocoagulation and intravitreous injection of SRPIN803. Expression levels of both MCP1 and ICAM1 were reduced by treatment with SRPIN803 (20 pmol/eye), relative to treatment with 0.1% DMSO (Fig. 5, C and D; $P < 0.05$). Thus, SRPIN803 suppressed both expression of inflammation-associated molecules and laser-induced neovascularization.

Treatment with Eye Ointment Containing SRPIN803. Intravitreous injection increases the risk of multiple complications. Therefore, we developed an eye ointment containing SRPIN803 at a final concentration of 10%. SRPIN803 was stable in the ointment for 4 weeks under various conditions (Supplemental Table 4). To determine whether topical administration of the ointment could suppress neovascularization, we administered it to model mice 3 times a day for 7 days after laser photocoagulation. Treatment with SRPIN803 ointment significantly decreased the neovascularization area, relative to treatment with substrate alone (Fig. 6, A and B; $P < 0.01$).

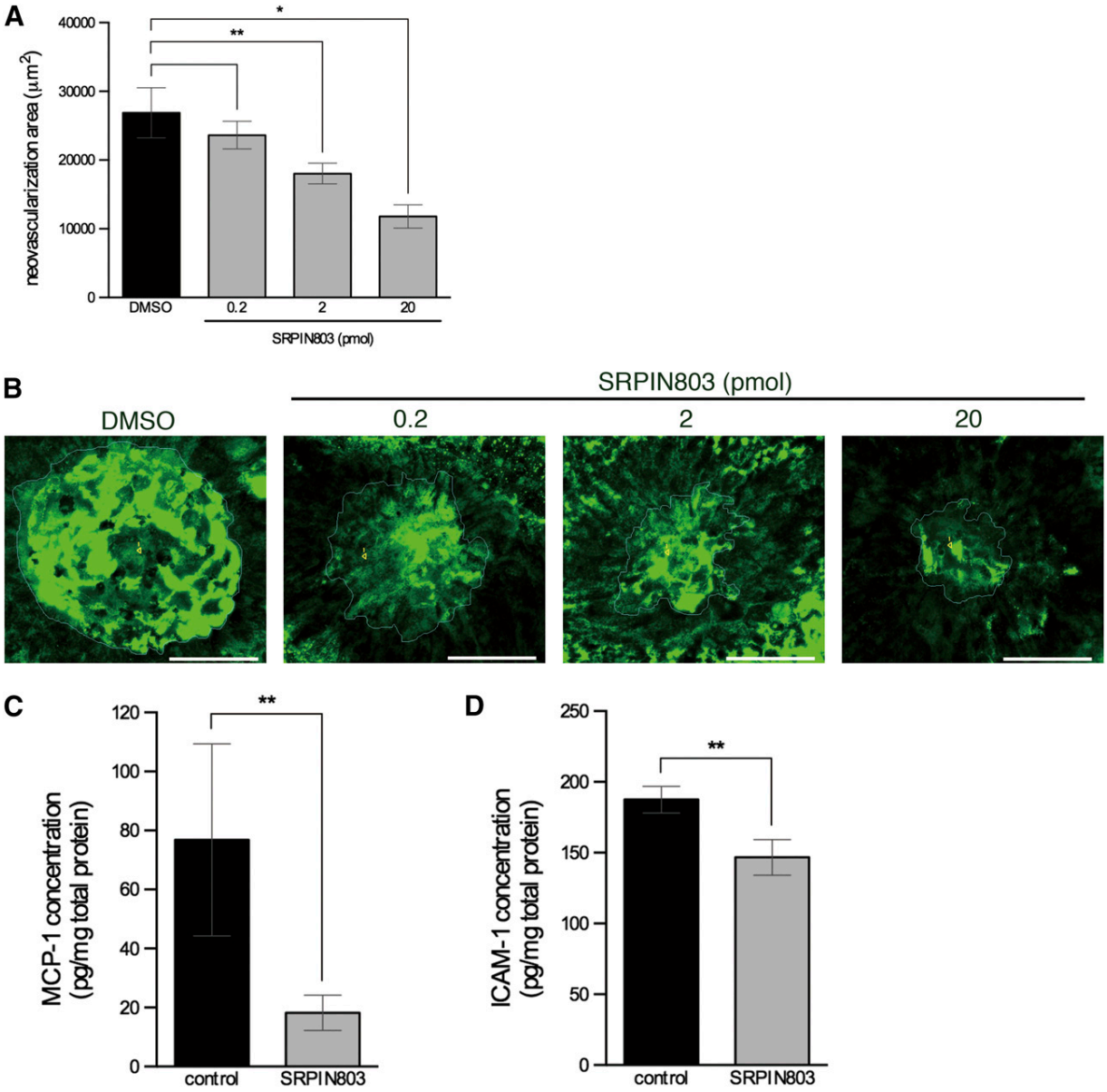

Fig. 5. SRPIN803 suppresses choroidal neovascularization in laser-induced model mice. (A and B) Intravitreous injection of SRPIN803 suppressed choroidal neovascularization. (A) Choroidal flat mounts were prepared from model mice 7 days after laser photocoagulation combined with intravitreous injection of 0.1% DMSO or SRPIN803 (0.20, 2.0, 20 pmol). The areas of choroidal neovascularization lesions in the flat mounts were quantitated [means ± S.E.M., n (number of neovascular lesions) = 17–26; $^{*}P < 0.01$; $^{**}P < 0.05$; $^{\dagger}P = 0.43$]. (B) Representative micrographs of neovascular lesions prepared in (A). Scale bar, 100 μm. (C and D) Reduction of inflammatory molecules by injection of SRPIN803. Bars indicate average protein levels of MCP1 (C) and ICAM1 (D) in retinal pigment epithelium and choroid obtained from model mice 3 days after laser photocoagulation combined with intravitreous injection of 0.1% DMSO or SRPIN803 (20 pmol). Protein levels were measured with enzyme-linked immunosorbent assay and normalized to total protein levels [means ± S.E.M., n (number of eyes) = 6; $^{**}P < 0.05$].

These data demonstrate that SRPIN803 has therapeutic activity, even in a topical ointment.

Discussion

In this study, we solved the crystal structure of the SRPK1/SRPIN340 complex. The structure revealed that SRPIN340 binds to the ATP-binding pocket and induces peptide flipping. On the basis of structural information, we screened a large-scale chemical library using an in silico virtual method followed by in vitro kinase assays. This screen identified SRPIN803, which was revealed to be a dual inhibitor of SRPK1 and CK2. The dual action of this drug efficiently suppressed VEGF production in the ARPE-19 cells. Furthermore, SRPIN803 suppressed choroidal neovascularization in model mice. Thus, SRPIN803 represents a promising candidate drug for treatment of neovascular diseases.

Peptide flipping induced by inhibitor binding to the pocket, which rearranges the hydrogen-bond network, has been demonstrated to enhance the inhibitor selectivity in mitogen-activated phosphatase and τ-tubulin kinase 1 (Fitzgerald et al., 2003; Nolen et al., 2003; Xue et al., 2013). SRPIN340

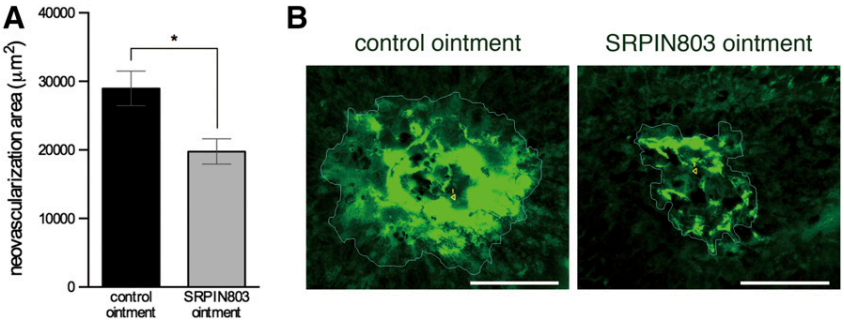

Fig. 6. SRPIN803 ointment suppresses choroidal neovascularization. (A and B) Treatment with ointment containing SRPIN803 (final concentration, 10%) suppressed choroidal neovascularization. (A) Quantitative analysis of the area of neovascularization [means ± S.E.M., n (number of neovascular lesions) = 18 for the control, n = 26 for SRPIN803; $^*P < 0.01$]. (B) Representative micrographs of neovascular lesions prepared in (A). Scale bar, 100 μm.

also induced peptide flipping in the pocket, a process in which the trifluoromethyl group of SRPIN340 may be involved. SRPIN803 also contains a trifluoromethyl group, positioned in the same way as that in the SRPK1/SRPIN340 complex, indicating that the trifluoromethyl group plays a critical role in selective inhibition of SRPK1. Data obtained using structural derivatives of SRPIN803 in which the trifluoromethyl group was replaced support the significance of this moiety to the drug's inhibitory activity.

Our group and others previously reported that SRPIN340 suppresses retinal neovascularization (Nowak et al., 2010; Gammons et al., 2013) and choroidal neovascularization (Dong et al., 2013) in model mice and rats. Furthermore, SRPIN340 and siRNA-mediated knockdown of *SRPK1* reduced VEGF-mediated tumor angiogenesis in metastatic melanoma (Gammons et al., 2014). In this study, we showed that the siRNA-mediated knockdown of *SRPK1* inhibited VEGF production, and that SRPIN803 suppressed choroidal neovascularization in model mice. Taken together, these data strongly support the idea that SRPK1 is a potential target for treatment of pathologic angiogenesis.

We showed previously that SRPIN340 suppressed *VEGF* mRNA expression in model mice (Dong et al., 2013). Here, we showed that *VEGF* mRNA expression was decreased in the ARPE-19 cells by either knockdown (si*SRPK1*) or treatment with SRPIN803. SRPIN803 inhibited not only SRPK1 but also CK2, an important regulator of hypoxia-inducible factor-1 activity that activates transcription of VEGF gene (Mottet et al., 2005). Inhibitors of CK2 decrease VEGF production in retinal pigmental epithelial cells (Mottet et al., 2005; Pollreisz et al., 2013), suppress proliferation and migration of retinal endothelial cells (Ljubimov et al., 2004), and decrease retinal neovascularization in mouse models of oxygen-induced retinopathy (Kramerov et al., 2008) and endometriotic lesions (Feng et al., 2012). Furthermore, siRNA-mediated knockdown of *CK2* decreased *VEGF* mRNA expression and VEGF protein level. Intravitreous injection of SRPIN803 suppressed choroidal neovascularization in model mice more effectively than SRPIN340, whereas the inhibitory activity of SRPIN803 against SRPK1 was weaker than that of SRPIN340. Because SRPIN340 did not inhibit CK2, this observation can be attributed to the dual inhibitory activity of SRPIN803.

This study indicated that VEGF production was decreased in ARPE-19 cells transfected with siRNAs of either *SRPK1* or *CK2*, and SRPIN803 decreased VEGF production through the inhibition of SRPK1 and/or CK2. Mylonis and Giannakouros, 2003 reported that CK2 phosphorylated and activated SRPK1. Whether these two kinases are involved in the regulation of VEGF production independently or not was previously unknown. Thus, further studies are required to understand how CK2 and SRPK1 regulate VEGF production.

Previous studies reported that repeated intravitreous injection of anti-VEGF drugs is associated with reduced bioefficacy (Schaal et al., 2008), and visual acuity has decreased in several percent of patients treated with existing anti-VEGF therapies (Martin et al., 2012). One potential explanation for this is that following treatment with anti-VEGF antibody the density of macrophages was higher in regions of choroidal neovascularization than in the absence of treatment (Tatar et al., 2008). Macrophages express VEGF within choroidal neovascularization (Grossniklaus et al., 2002), and this expression is related to the severity of choroidal neovascularization (Espinosa-Heidmann et al., 2003; Sakurai et al., 2003). In this study, SRPIN803 reduced the protein level of MCP1, which plays a role in macrophage recruitment (Salcedo et al., 2000). Thus, MCP1 suppression by SRPIN803 may contribute to the drug's potent in vivo effect.

This study identified a dual inhibitor of SRPK1 and CK2, SRPIN803, as a potential drug candidate for therapies against neovascular diseases. Treatment with SRPIN803 did not cause cytotoxicity in ARPE-19 cells. Furthermore, administration of the drug either by intravitreous injection or as a topical ointment suppressed choroidal neovascularization in the model mice. In AMD patients, the route of administration for anti-VEGF antibodies is limited to intravitreous injection, which imposes a burden on both patients and doctors because of the elevated risk of several complications. Our findings suggest that SRPIN803 could contribute to avoidance of this risk.

Anti-VEGF antibodies have also been approved not only for other intraocular neovascular diseases, such as retinal vein occlusion and diabetic retinopathy, but also for various cancers, including colorectal cancer, lung cancer, and glioblastoma. It is possible that SRPIN803 could have an effect on these neovascular diseases. Overall, the findings reported here indicate that SRPIN803 represents a novel anti-VEGF agent for use in clinical therapeutics.

Acknowledgments

The authors thank Souhei Matsushita (Tokyo Medical and Dental University) for crystal structure analyses, and Manami Sasaki (Kyoto University), Sayaka Matsumura (Kyoto University), and Dr. Kenji Suda (Kyoto University) for technical assistance. The authors also thank the Institute of Laboratory Animals of Kyoto University for critical assistance with animal experiments, and the Radioisotope Research Center of Kyoto University for critical assistance with the radioisotope experiments.

Authorship Contributions

Participated in research design: Morooka, Kii, Yoshimura, Hagiwara.

Conducted experiments: Morooka, Denawa, Ninomiya, Fukuhara, Noda, Ishida.

Contributed new reagents or analytic tools: Hoshina, Okabe, Kojima, Inoue, Okuno, Ikura, Furuya, Nagano, Hosoya, Ito.

Performed data analysis: Morooka, Denawa.

Wrote or contributed to the writing of the manuscript: Morooka, Kii, Hosoya, Ito, Hagiwara.

References

Aguilar E, Dorrell MI, Friedlander D, Jacobson RA, Johnson A, Marchetti V, Moreno SK, Ritter MR, and Friedlander M (2008) Chapter 6. Ocular models of angiogenesis. *Methods Enzymol* **444**:115–158.

Amin EM, Oltean S, Hua J, Gammons MV, Hamdollah-Zadeh M, Welsh GI, Cheung MK, Ni L, Kase S, and Rennel ES et al. (2011) WT1 mutants reveal SRPK1 to be a downstream angiogenesis target by altering VEGF splicing. *Cancer Cell* **20**: 768–780.

Baell JB and Holloway GA (2010) New substructure filters for removal of pan assay interference compounds (PAINS) from screening libraries and for their exclusion in bioassays. *J Med Chem* **53**:2719–2740.

Daub H, Blencke S, Habenberger P, Kurtenbach A, Dennenmoser J, Wissing J, Ullrich A, and Cotten M (2002) Identification of SRPK1 and SRPK2 as the major cellular protein kinases phosphorylating hepatitis B virus core protein. *J Virol* **76**: 8124–8137.

De Moliner E, Moro S, Sarno S, Zagotto G, Zanotti G, Pinna LA, and Battistutta R (2003) Inhibition of protein kinase CK2 by anthraquinone-related compounds. A structural insight. *J Biol Chem* **278**:1831–1836.

Dong Z, Noda K, Kanda A, Fukuhara J, Ando R, Murata M, Saito W, Hagiwara M, and Ishida S (2013) Specific inhibition of serine/arginine-rich protein kinase attenuates choroidal neovascularization. *Mol Vis* **19**:536–543.

Dulak J, Deshane J, Jozkowicz A, and Agarwal A (2008) Heme oxygenase-1 and carbon monoxide in vascular pathobiology: focus on angiogenesis. *Circulation* **117**: 231–241.

Emsley P, Lohkamp B, Scott WG, and Cowtan K (2010) Features and development of Coot. *Acta Crystallogr D Biol Crystallogr* **66**:486–501.

Espinosa-Heidmann DG, Suner IJ, Hernandez EP, Monroy D, Csaky KG, and Cousins SW (2003) Macrophage depletion diminishes lesion size and severity in experimental choroidal neovascularization. *Invest Ophthalmol Vis Sci* **44**: 3586–3592.

Feng D, Welker S, Körbel C, Rudzitis-Auth J, Menger MD, Montenarh M, and Laschke MW (2012) Protein kinase CK2 is a regulator of angiogenesis in endometriotic lesions. *Angiogenesis* **15**:243–252.

Ferrara N, Gerber HP, and LeCouter J (2003) The biology of VEGF and its receptors. *Nat Med* **9**:669–676.

Ferris FL, 3rd, Fine SL, and Hyman L (1984) Age-related macular degeneration and blindness due to neovascular maculopathy. *Arch Ophthalmol* **102**:1640–1642.

Fitzgerald CE, Patel SB, Becker JW, Cameron PM, Zaller D, Pikounis VB, O'Keefe SJ, and Scapin G (2003) Structural basis for p38alpha MAP kinase quinazolinone and pyridol-pyrimidine inhibitor specificity. *Nat Struct Biol* **10**:764–769.

Fukuda R, Hirota K, Fan F, Jung YD, Ellis LM, and Semenza GL (2002) Insulin-like growth factor 1 induces hypoxia-inducible factor 1-mediated vascular endothelial growth factor expression, which is dependent on MAP kinase and phosphatidylinositol 3-kinase signaling in colon cancer cells. *J Biol Chem* **277**:38205–38211.

Fukuhara T, Hosoya T, Shimizu S, Sumi K, Oshiro T, Yoshinaka Y, Suzuki M, Yamamoto N, Herzenberg LA, and Herzenberg LA et al. (2006) Utilization of host SR protein kinases and RNA-splicing machinery during viral replication. *Proc Natl Acad Sci USA* **103**:11329–11333.

Gammons MV, Dick AD, Harper SJ, and Bates DO (2013) SRPK1 inhibition modulates VEGF splicing to reduce pathological neovascularization in a rat model of retinopathy of prematurity. *Invest Ophthalmol Vis Sci* **54**:5797–5806.

Gammons MV, Lucas R, Dean R, Coupland SE, Oltean S, and Bates DO (2014) Targeting SRPK1 to control VEGF-mediated tumour angiogenesis in metastatic melanoma. *Br J Cancer* **111**:477–485.

Gragoudas ES, Adamis AP, Cunningham ET, Jr, Feinsod M, and Guyer DR VEGF Inhibition Study in Ocular Neovascularization Clinical Trial Group (2004) Pegaptanib for neovascular age-related macular degeneration. *N Engl J Med* **351**: 2805–2816.

Grossniklaus HE, Ling JX, Wallace TM, Dithmar S, Lawson DH, Cohen C, Elner VM, Elner SG, and Sternberg P, Jr (2002) Macrophage and retinal pigment epithelium expression of angiogenic cytokines in choroidal neovascularization. *Mol Vis* **8**: 119–126.

Hathaway GM and Traugh JA (1982) Casein kinases—multipotential protein kinases. *Curr Top Cell Regul* **21**:101–127.

Heier JS, Brown DM, Chong V, Korobelnik JF, Kaiser PK, Nguyen QD, Kirchhof B, Ho A, Ogura Y, and Yancopoulos GD et al.; VIEW 1 and VIEW 2 Study Groups (2012) Intravitreal aflibercept (VEGF trap-eye) in wet age-related macular degeneration. *Ophthalmology* **119**:2537–2548.

Hu SI, Katz M, Chin S, Qi X, Cruz J, Ibebunjo C, Zhao S, Chen A, and Glass DJ (2012) MNK2 inhibits eIF4G activation through a pathway involving serine-arginine-rich protein kinase in skeletal muscle. *Sci Signal* **5**:ra14.

Hurwitz H, Fehrenbacher L, Novotny W, Cartwright T, Hainsworth J, Heim W, Berlin J, Baron A, Griffing S, and Holmgren E et al. (2004) Bevacizumab plus irinotecan, fluorouracil, and leucovorin for metastatic colorectal cancer. *N Engl J Med* **350**:2335–2342.

Klein R, Wang Q, Klein BE, Moss SE, and Meuer SM (1995) The relationship of age-related maculopathy, cataract, and glaucoma to visual acuity. *Invest Ophthalmol Vis Sci* **36**:182–191.

Kramerov AA, Saghizadeh M, Caballero S, Shaw LC, Li Calzi S, Bretner M, Montenarh M, Pinna LA, Grant MB, and Ljubimov AV (2008) Inhibition of protein kinase CK2 suppresses angiogenesis and hematopoietic stem cell recruitment to retinal neovascularization sites. *Mol Cell Biochem* **316**:177–186.

Lin J, Handschin C, and Spiegelman BM (2005) Metabolic control through the PGC-1 family of transcription coactivators. *Cell Metab* **1**:361–370.

Litchfield DW (2003) Protein kinase CK2: structure, regulation and role in cellular decisions of life and death. *Biochem J* **369**:1–15.

Ljubimov AV, Caballero S, Aoki AM, Pinna LA, Grant MB, and Castellon R (2004) Involvement of protein kinase CK2 in angiogenesis and retinal neovascularization. *Invest Ophthalmol Vis Sci* **45**:4583–4591.

Maharaj AS and D'Amore PA (2007) Roles for VEGF in the adult. *Microvasc Res* **74**: 100–113.

Martin D, Galisteo R, and Gutkind JS (2009) CXCL8/IL8 stimulates vascular endothelial growth factor (VEGF) expression and the autocrine activation of VEGFR2 in endothelial cells by activating NFkappaB through the CBM (Carma3/Bcl10/Malt1) complex. *J Biol Chem* **284**:6038–6042.

Martin DF, Maguire MG, Fine SL, Ying GS, Jaffe GJ, Grunwald JE, Toth C, Redford M, and Ferris FL, 3rd Comparison of Age-related Macular Degeneration Treatments Trials (CATT) Research Group (2012) Ranibizumab and bevacizumab for treatment of neovascular age-related macular degeneration: two-year results. *Ophthalmology* **119**:1388–1398.

Meggio F and Pinna LA (2003) One-thousand-and-one substrates of protein kinase CK2? *FASEB J* **17**:349–368.

Meisner H, Heller-Harrison R, Buxton J, and Czech MP (1989) Molecular cloning of the human casein kinase II alpha subunit. *Biochemistry* **28**:4072–4076.

Mottet D, Ruys SP, Demazy C, Raes M, and Michiels C (2005) Role for casein kinase 2 in the regulation of HIF-1 activity. *Int J Cancer* **117**:764–774.

Murshudov GN, Skubák P, Lebedev AA, Pannu NS, Steiner RA, Nicholls RA, Winn MD, Long F, and Vagin AA (2011) REFMAC5 for the refinement of macromolecular crystal structures. *Acta Crystallogr D Biol Crystallogr* **67**:355–367.

Mylonis I and Giannakouros T (2003) Protein kinase CK2 phosphorylates and activates the SR protein-specific kinase 1. *Biochem Biophys Res Commun* **301**:650–656.

Ngo JC, Chakrabarti S, Ding JH, Velazquez-Dones A, Nolen B, Aubol BE, Adams JA, Fu XD, and Ghosh G (2005) Interplay between SRPK and Clk/Sty kinases in phosphorylation of the splicing factor ASF/SF2 is regulated by a docking motif in ASF/SF2. *Mol Cell* **20**:77–89.

Ngo JC, Gullingsrud J, Giang K, Yeh MJ, Fu XD, Adams JA, McCammon JA, and Ghosh G (2007) SR protein kinase 1 is resilient to inactivation. *Structure* **15**:123–133.

Nikolakaki E, Drosou V, Sanidas I, Peidis P, Papamarcaki T, Iakoucheva LM, and Giannakouros T (2008) RNA association or phosphorylation of the RS domain prevents aggregation of RS domain-containing proteins. *Biochim Biophys Acta* **1780**:214–225.

Nishida A, Kataoka N, Takeshima Y, Yagi M, Awano H, Ota M, Itoh K, Hagiwara M, and Matsuo M (2011) Chemical treatment enhances skipping of a mutated exon in the dystrophin gene. *Nat Commun* **2**:308.

Nolen B, Ngo J, Chakrabarti S, Vu D, Adams JA, and Ghosh G (2003) Nucleotide-induced conformational changes in the Saccharomyces cerevisiae SR protein kinase, Sky1p, revealed by X-ray crystallography. *Biochemistry* **42**:9575–9585.

Nowak DG, Amin EM, Rennel ES, Hoareau-Aveilla C, Gammons M, Damodoran G, Hagiwara M, Harper SJ, Woolard J, and Ladomery MR et al. (2010) Regulation of vascular endothelial growth factor (VEGF) splicing from pro-angiogenic to anti-angiogenic isoforms: a novel therapeutic strategy for angiogenesis. *J Biol Chem* **285**:5532–5540.

Noy P, Gaston K, and Jayaraman PS (2012a) Dasatinib inhibits leukaemic cell survival by decreasing PRH/Hhex phosphorylation resulting in increased repression of VEGF signalling genes. *Leuk Res* **36**:1434–1437.

Noy P, Sawasdichai A, Jayaraman PS, and Gaston K (2012b) Protein kinase CK2 inactivates PRH/Hhex using multiple mechanisms to de-repress VEGF-signalling genes and promote cell survival. *Nucleic Acids Res* **40**:9008–9020.

Ogawa Y and Hagiwara M (2012) Challenges to congenital genetic disorders with "RNA-targeting" chemical compounds. *Pharmacol Ther* **134**:298–305.

Okabe K, Kobayashi S, Yamada T, Kurihara T, Tai-Nagara I, Miyamoto T, Mukouyama YS, Sato TN, Suda T, and Ema M et al. (2014) Neurons limit angiogenesis by titrating VEGF in retina. *Cell* **159**:584–596.

Olsten ME and Litchfield DW (2004) Order or chaos? An evaluation of the regulation of protein kinase CK2. *Biochem Cell Biol* **82**:681–693.

Pinna LA (1990) Casein kinase 2: an 'eminence grise' in cellular regulation? *Biochim Biophys Acta* **1054**:267–284.

Pollreisz A, Afonyushkin T, Oskolkova OV, Gruber F, Bochkov VN, and Schmidt-Erfurth U (2013) Retinal pigment epithelium cells produce VEGF in response to oxidized phospholipids through mechanisms involving ATF4 and protein kinase CK2. *Exp Eye Res* **116**:177–184.

Rosenfeld PJ, Brown DM, Heier JS, Boyer DS, Kaiser PK, Chung CY, and Kim RY; MARINA Study Group (2006) Ranibizumab for neovascular age-related macular degeneration. *N Engl J Med* **355**:1419–1431.

Sakurai E, Anand A, Ambati BK, van Rooijen N, and Ambati J (2003) Macrophage depletion inhibits experimental choroidal neovascularization. *Invest Ophthalmol Vis Sci* **44**:3578–3585.

Salcedo R, Ponce ML, Young HA, Wasserman K, Ward JM, Kleinman HK, Oppenheim JJ, and Murphy WJ (2000) Human endothelial cells express CCR2 and respond to MCP-1: direct role of MCP-1 in angiogenesis and tumor progression. *Blood* **96**:34–40.

Schaal S, Kaplan HJ, and Tezel TH (2008) Is there tachyphylaxis to intravitreal anti-vascular endothelial growth factor pharmacotherapy in age-related macular degeneration? *Ophthalmology* **115**:2199–2205.

Seddon JM and Chen CA (2004) The epidemiology of age-related macular degeneration. *Int Ophthalmol Clin* **44**:17–39.

Shima C, Sakaguchi H, Gomi F, Kamei M, Ikuno Y, Oshima Y, Sawa M, Tsujikawa M, Kusaka S, and Tano Y (2008) Complications in patients after intravitreal injection of bevacizumab. *Acta Ophthalmol (Copenh)* **86**:372–376.

Tatar O, Yoeruek E, Szurman P, Bartz-Schmidt KU, Adam A, Shinoda K, Eckardt C, Boeyden V, Claes C, and Pertile G et al.; Tübingen Bevacizumab Study Group (2008) Effect of bevacizumab on inflammation and proliferation in human choroidal neovascularization. *Arch Ophthalmol* **126**:782–790.

Trott O and Olson AJ (2010) AutoDock Vina: improving the speed and accuracy of docking with a new scoring function, efficient optimization, and multithreading. *J Comput Chem* **31**:455–461.

Unger GM, Davis AT, Slaton JW, and Ahmed K (2004) Protein kinase CK2 as regulator of cell survival: implications for cancer therapy. *Curr Cancer Drug Targets* **4**:77–84.

Ventrice P, Leporini C, Aloe JF, Greco E, Leuzzi G, Marrazzo G, Scorcia GB, Bruzzichesi D, Nicola V, and Scorcia V (2013) Anti-vascular endothelial growth factor drugs safety and efficacy in ophthalmic diseases. *J Pharmacol Pharmacother* **4**:S38–42.

Wang P, Zhou Z, Hu A, Ponte de Albuquerque C, Zhou Y, Hong L, Sierecki E, Ajiro M, Kruhlak M, and Harris C et al. (2014) Both decreased and increased SRPK1 levels promote cancer by interfering with PHLPP-mediated dephosphorylation of Akt. *Mol Cell* **54**:378–391.

Winn MD, Ballard CC, Cowtan KD, Dodson EJ, Emsley P, Evans PR, Keegan RM, Krissinel EB, Leslie AG, and McCoy A et al. (2011) Overview of the CCP4 suite and current developments. *Acta Crystallogr D Biol Crystallogr* **67**:235–242.

Wolf A, Agnihotri S, Micallef J, Mukherjee J, Sabha N, Cairns R, Hawkins C, and Guha A (2011) Hexokinase 2 is a key mediator of aerobic glycolysis and promotes tumor growth in human glioblastoma multiforme. *J Exp Med* **208**: 313–326.

Xu J, Liu X, Jiang Y, Chu L, Hao H, Liua Z, Verfaillie C, Zweier J, Gupta K, and Liu Z (2008) MAPK/ERK signalling mediates VEGF-induced bone marrow stem cell differentiation into endothelial cell. *J Cell Mol Med* **12** (6A):2395–2406.

Xue Y, Wan PT, Hillertz P, Schweikart F, Zhao Y, Wissler L, and Dekker N (2013) X-ray structural analysis of tau-tubulin kinase –1 and its interactions with small molecular inhibitors. *ChemMedChem* **8**:1846–1854.

Address correspondence to: Dr. Masatoshi Hagiwara, Department of Anatomy and Developmental Biology, Graduate School of Medicine, Kyoto University, Yoshida-Konoe-cho, Sakyo-ku, Kyoto 606-8501, Japan. E-mail: hagiwara.masatoshi.8c@kyoto-u.ac.jp